# Molecular simulation of silica gels: Formation, dilution, and drying

Romain Dupuis,[1,*] Laurent Karim Béland,[2] and Roland J.-M. Pellenq[1]

[1]*CNRS/MIT/Aix-Marseille Université Joint Laboratory "MultiScale Materials Science for Energy and Environment," UMI <MSE>2, Massachusetts Institute of Technology, 77 Massachusetts Avenue, Cambridge, Massachusetts 02139, USA*

[2]*Department of Mechanical and Materials Engineering, Queen's University, 99 University Ave, Kingston, Ontario, Canada K7L 3N6*

(Received 25 February 2019; revised manuscript received 28 May 2019; published 17 July 2019)

The formation and ageing of gels is a complex issue that has to be resolved to investigate manifold synthetic materials, among them: porous materials such as cement, high-quality glass fiber, and geomaterials for radioactive waste sealing. Herein, a coupling between a grand canonical Monte Carlo and the parallel tempering methods is developed. The gain in simulation time is of, at least, two orders of magnitude; therefore, we are able to move at will on the water to silicon ratio axis and to observe the restructuring of gels during dilution and drying. At high water to silicon ratio, a colloidal-like structure is obtained, mostly constituted of silicate chains. As humidity is an essential aspect of gels, affecting their physical and mechanical properties, the effect of drying is herein investigated. In agreement with experiments, the structure becomes denser, crosslinks between silicate chains increase and glasslike structures are observed locally.

DOI: 10.1103/PhysRevMaterials.3.075603

## I. INTRODUCTION

Understanding the formation of gel-like structures is an important contemporary research topic [1–10]. In gels, water plays an essential role since gels of low hydration exhibit glassy behavior [11] and gels of high hydration become softer. Given their disordered structure, experimentally investigation their formation and different stages of life is challenging. Gels are nowadays used in the production of a variety of materials. Knowing the structural, mechanical and dynamical properties of gels would have far-reaching consequences, which include improving the synthesis and lengthening the lifetime of these materials [8]. In this paper, we focused on the following question: as hydration conditions vary, how does the atomistic structure of a silica gel change?

The aforementioned knowledge would be of great help in the following six contexts. First, in the widely used sol-gel technique, colloids are agglomerated in a liquid and then dehydrated to synthesize materials such as high-quality fiberglass, silicate materials including zeolites, and bioactive glasses [9,12]. Second, in order to prevent degradation of the containment matrix during radioactive waste sequestration in glasses or cement [13], silica glasses are partly dissolved through hydration. The dissolved glass forms a gel layer that passivates the surface and hampers oxidation [14]. Third, glass makers wet glass surfaces before cutting in order to reduce the material's resistance and preserve its integrity. Fourth, cement, the most abundantly produced man-made material is a porous substance mostly composed of a calcium-silicate-hydrate gel. Its production is associated with 8% of the world's greenhouse gas emissions. Optimizing its synthesis and lifetime could improve its carbon footprint [15,16]. Another notable challenge for concrete is avoiding the appearance of cracks due to the delayed formation of alkali-silica gels [17] in its pores. Fifth, in addition to its use to synthesize materials, precipitations occurs in nature and are sometimes initiated by precursors that are gel-like colloidal solutions [18,19]. Finally, gels are now used for medical applications. Among those, biogels can serve to encapsulate drugs in order to continuously dispatch the drug in the body [20]. Biogels could also be used to produce biomaterials for 3D printing organs [21] for which a key concern is their fatigue resistance.

The broad range of fields where this understanding would be of value, coupled to the dearth of information pertaining to the nanostructure of gels, has led to modeling these gels by atomistic simulations [9,22–25]. A promising approach to observe the formation of silicate gels is to consider a liquid phase and to run molecular dynamics simulations at high temperature for long durations [9,23]. Melts were also been considered, which tend to be closer to the final gel structure [26,27]. It has also been proposed to randomly remove bonds in a silica glass and fill thus formed pores with water molecules [28]. Realistically simulating the formation of gels requires rather demanding computational power. Gels have weak long-distance ordering and gelation is a slow process due to a high-energy barrier for siloxane bond formation—the activation energy for two monomers was experimentally and theoretically determined to be 0.1–0.6 eV [8,23].

To better describe the gelation process and control hydration, we developed a method that couples grand canonical Monte Carlo (GCMC) and brief parallel tempering (brief-PT). The GCMC simulation allows the addition or removal of water molecules and mimics the formation of gels in liquids. The chemical potential is a parameter to adjust water concentration. The brief-PT enhances silicate bond formation and reduces computational costs. Using this cost-efficient method, we were able to study the formation of silica gels.

*rdupuis@mit.edu

 

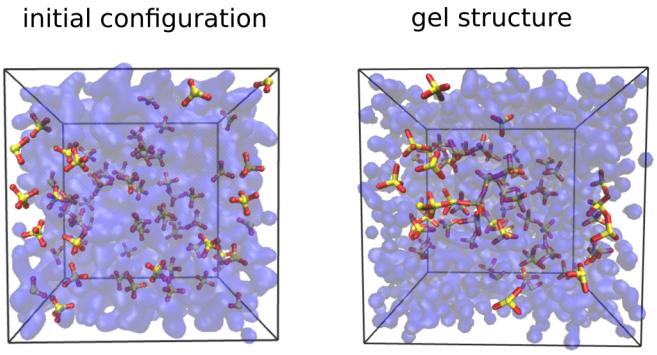


FIG. 1. An illustration of a typical starting configuration before melting (left) and of a typical configuration after the GCMC-PT procedure (right). Silicon, oxygen, and hydrogen atoms are represented in yellow, red, and white spheres, respectively. The transparent blue volume drapes the water molecules.

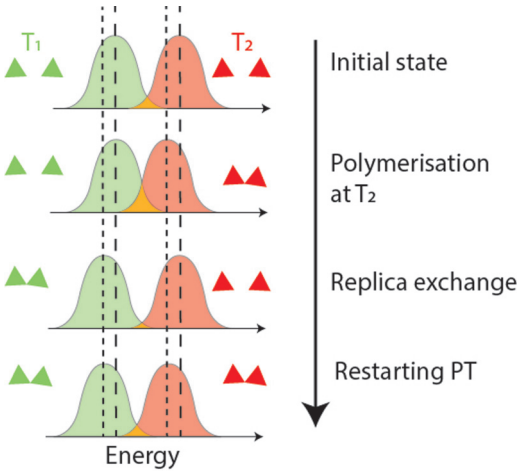


FIG. 2. Brief-PT algorithm. Energy distribution for a given temperature and state. Orange area corresponds to the overlap. Green and red triangles represent two simplified states of the polymerisation (two monomers or dimers).

## II. METHODS

The starting point of the simulation is a liquid in which silicon is composed only of $Si(OH)_4$ silicate monomers, as shown in Fig. 1. In the rest of the manuscript, monomers will refer to $SiO_4H_x$, were $x$ is the degree of protonation. The liquid has the composition foreseen for the gel. In order to simulate the gelation of the liquid, it is necessary to take into account the dissociation of water molecules and the bond formation for silicon and oxygen atoms. Hereafter, we consider that a Si-O bond is formed using a cutoff of 2.0 Å that corresponds to the first minimum in the radial distribution function. Chemical reactions are enable by reactive force fields—i.e., REAXFF [29] using the parameters provided in Psofogiannakis *et al.* [30,31]. Then, we start a phase where GCMC and brief-PT are alternatively applied. In GCMC, the quantity of water is equilibrated with a chemical potential. PT [32,33] accelerates the formation of silicate chains. Parallel tempering—also called replica exchange—is a method in which run several simulations are run at different temperatures. In PT, after a given number of steps, the configurations can swap with a probability given by their thermodynamic weights. High-temperature replica are more likely to cross energy barriers and form bonds. This enhances the crossing of high-energy barriers. The simulation loops over these two steps until the gel is formed. A new aspect of the methodology presented in this work is repeating brief-PT simulations in order to hasten the convergence of the structure.

In PT, if the new configuration obtained at high temperature is of higher stability, its energy will decrease and the probability of accepting the swap with a lower temperature configuration increases (see Fig. 2). If this exchange is accepted, the probability of exchange will be lowered significantly because now the structure of higher stability is at low temperature. A perk of the proposed method is that brief-PT enhances the convergence to the final structure, in comparison to regular PT. This originates from the fact that when the PT is interrupted, the configuration obtained at low temperature—that eventually originates from an exchange with higher-temperature simulation—will be preserved and used as a restarting configuration for all temperatures in the next loop, as shown in Fig. 2(d). In brief-PT, the lowest energy state periodically repopulate the ensemble of the replica. As shown in Fig. 3, this corresponds to an increase of two orders of magnitude during the condensation of monomers into dimers. The gain is even greater during the formation of more complex structures containing $Q_3$. Indeed, the brief-PT method will be more beneficial for bonds that are less likely to be made–either because the frequency of attempts is low or because the energy barrier is high. As shown hereafter, brief-PT allows both bond formation and bond dissociation and can quickly reproduce the effect of dilution or drying of the gels.

For pure silicate, the composition $2HSi_2O_5 \cdot nH_2O$ was used, where the number of water molecules $N_{H_2O}$ is a variable during the GCMC step. In details, initial liquid configurations are made of an array of unit cells duplicated to obtain a cell of $35 \times 30 \times 15$ Å$^3$ that contains 100 silicate monomers and a variable number of water molecules. For 64 silicon atoms and more, it has been shown that there is no significant size effect [9]. Note that at scales of 30 Å and more gels might show a weak long distance ordering due to formation of large-size clusters. We have used time steps of 0.1 fs. The coupling of Parallel tempering and GCMC starts with 10 GCMC trials which are separated by 10 fs of a NVT ensemble molecular dynamics—this constitutes the GCMC step. Our GCMC trial move includes not only an insertion/deletion—as is traditionally done—but also a short MD relaxation run. The acceptance/rejection of the trial move is done on the basis of the Boltzmann-weighted difference in energy between the states before and after the trial move–i.e., before and after the insertion/deletion+MD. This allows water molecules and their surrounding structures to diffuse and re-arrange in order to form lower energy configurations before accepting or refusing the move. These trial moves are more expensive than traditional GCMC trial moves, but yield a higher acceptance probability, which leads to an efficient exploration of phase space. Doing so, we are leaving the possibility for the water molecules to diffuse to a lower energy site before accepting or refusing the move. For each trial, a metropolis criteria is calculated, and the addition or removal of water molecules is

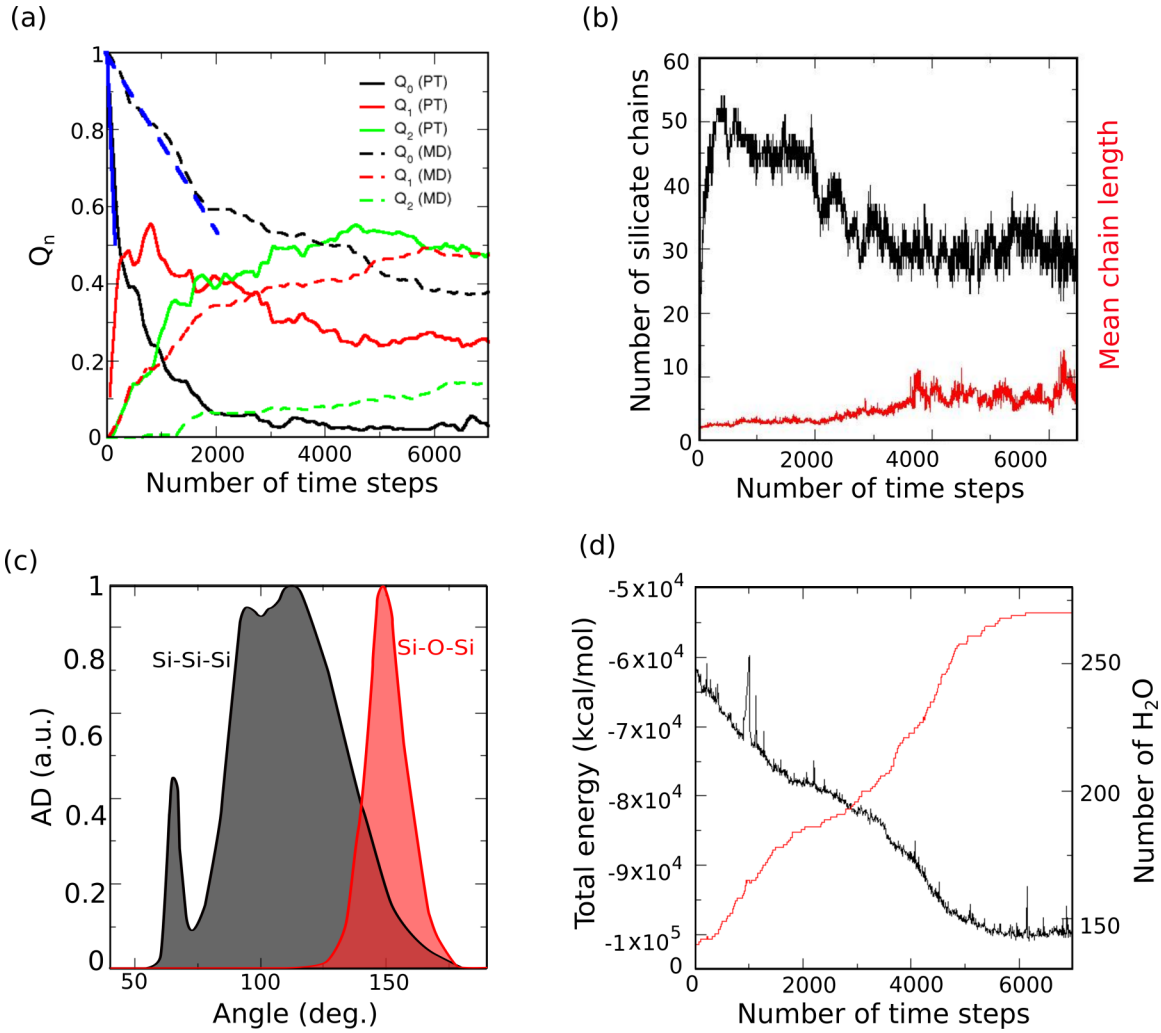


FIG. 3. (a) Evolution of $Q_n$ during the first steps of the formation of a calcium silicate hydrate gel using the GCMC + PT method (full lines) or a classical MD performed at 2000 K (dashed lines). $Q_3$ and $Q_4$ are omitted for clarity. The consumption of $Q_0$ is increased by two orders of magnitude in PT. (b) Number of silicate chains and mean chain length. (c) Angular distribution function after gelation. (d) Variation of the total energy of the system and of the amount of water molecules in the system.

accepted or rejected according to the chemical potential for a water molecule in the bulk. The value of $\mu_{H_2O}$ was previously calculated by simulating bulk water using REAXFF. We found a value of 225 kcal/mol and we tested that the number of water molecules was conserved at density 1. Other values of $\mu_{H_2O}$ were also used to force hydration or drying of the system. The simulation continues with 500 parallel tempering steps with a chosen ratio of permutation attempts over NVT molecular dynamics steps of 1/10 and then the simulation loops to the GCMC step. A set of 16 temperatures were chosen ranging from 300 to 1000 K and we verified that the replica are switched regularly (about 10% of the attempts were successful). This method has been thought to simulate the wet environment during the gel formation in the pores of concrete and allow water addition or removal. It also accounts for slow gelation due to the energy barrier of about 15 kcal/mol for the formation of siloxanes. Hereafter, the structures that are being studied are pure silica gels. The effects of chemical change and water concentration are investigated using the aforementioned GCMC + PT coupling.

## III. RESULTS AND DISCUSSION

### A. Gelation

Gelation starts with consumption of silicate monomers ($Q_0$) to quickly form dimers ($Q_1$). $Q_n$ corresponds to the number of bridging oxygen around a silicon atom. Later the polymerization of the silicate chains continues with the appearance of $Q_2$ silicon which corresponds to the formation of silicate chains made with three silicon atoms or more. The comparison of the GCMC + PT method with a high-temperature classical molecular dynamics in Fig. 3 shows an increase in the speed of the formation of the gel by two orders of magnitude. This is emphasized in Fig. 3 by the blue lines that correspond to the initial slopes of the consumption of silicate monomers ($Q_0$) to form the first dimers. The gain in speed for forming the gels largely compensates for the additional costs of the method which is about 16 times more costly relative to classical MD. During the simulation, the mean chain length increases (see Fig. 3). The gel forms by the polycondensation of silicate chains that form a rigid

body that embeds water. As for $Q_n$, the length of the chain converges and spans from monomers to silicate chains of more than 15 silicon atoms. During the gelation, few rings were formed as observed experimentally in glasses [34]. The ring repartition is the following: 6 rings has been formed, with two five-member rings, one four-member ring, and three three-member rings. The angular distribution function for Si–O–Si angles shows a peak at 145°, which is in agreement with DFT calculations that give an angle of about 141° and other empirical calculations with empirical potentials [35]. The Si–Si–Si angular distribution has a bimodal shape. The first peak, centered on 60°, corresponds to Si atoms located in ring patterns whereas, the one around 120° corresponds Si atoms in a chain.

The total energy of the system depends on the number of atoms (which varies during the GCMC steps) and on the structure of the gel during the dynamics. In the simulations, the energy converged after about 5000 steps [Fig. 3(a)]. At the same time, the number of water molecules rose to about 280 which corresponds to a ratio $N_{\text{water}}/N_{\text{Si}}$ of 2. Gelation tends to favor adsorption of water molecules in part because during the polycondensation of the silicate chains, there are low-density spaces in the simulation box. Water is added in these recently formed empty nanopores. This phenomenon implies demixing of water molecules with the silicate structure.

The efficient method used above has accelerated the condensation of monomers into dimers by at least to orders of magnitude. The structures can be compared with experiments such as nuclear magnetic resonance (NMR), infrared spectroscopy and Raman spectroscopy that has been conducted on silica and ASR gels [36–38]. NMR is an essential guide to determine what could be silicate chain length and assemblage (single chains, double chains, rings, etc.) [39]. In these experiments, the gels mostly have Q2 and Q3 units which most likely indicates that the silicate chains in the gel are long. In our simulations, we observed that the hydration affects the proportion of $Q_n$. The ratio of the number of bridging oxygen atoms (BO) divided by the number of silicon atoms gives information on the structure of the gels and can be calculated simply using $Q_n$ information:

$$N_{\text{BO}}/N_{\text{Si}} = (Q_1 + 2Q_2 + 3Q_3 + 4Q_4)/(2N_{\text{Si}}). \quad (1)$$

Hereafter, we present the results we obtained for the gelation, followed by a dilution and a drying of the gel as shown in Fig. 4. For the pure silicate gel, we found that $N_{\text{BO}}/N_{\text{Si}}$ varies with the dilution level which is in agreement with experimental data [40]. The simulation started with a ratio $N_{\text{water}}/N_{\text{Si}}$ of 1.5 which is relatively low and we found that $N_{\text{BO}}/N_{\text{Si}}$ converges to 0.88.

### B. Dilution

On the second stage of the simulation, with a hydration ratio $N_{\text{water}}/N_{\text{Si}}$ equals 3, $N_{\text{BO}}/N_{\text{Si}}$ changes to 0.65, which corresponds to previous results obtained by molecular dynamics at high temperature [9]. This indicates that using the parallel tempering technique, the system swiftly crosses high-energy barriers and preserves the correct chemistry to form the silicate chains. The number of monomers suddenly increases to reach the double of its initial value. Meanwhile,

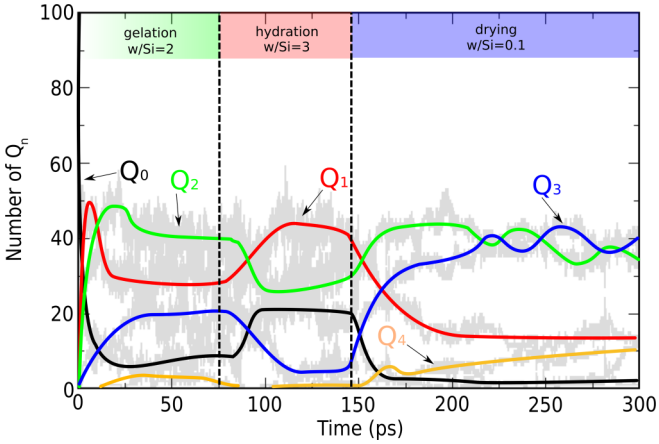


FIG. 4. Evolution of $Q_n$ during gelation (w/Si = 1), dilution(w/Si = 3), and drying (w/Si = 0.1). Gray lines corresponds to instantaneous values of $Q_n$ calculated along the trajectory. Black, red, green, blue, and orange lines are guide for the eyes that represents the evolution of $Q_0$, $Q_1$, $Q_2$, $Q_3$, and $Q_4$, respectively.

all $Q_4$ are dissociated and $Q_2$ and $Q_3$ numbers drop. The hydrolysis of the silicate chains is conjugated by the demixing of water. Added water molecules will drive away the silica chains. Therefore the probability of forming crosslinks between chains decreases and the effect of dissociation prevails, leading to the release of $Q_0$. The fact that we observe an increase or a decrease of $N_{\text{BO}}/N_{\text{Si}}$ while we add or remove water molecules is an indicator of the remarkable ability of the simulation to realistically reproduce the properties of a gel. This is possible because siloxane bonds are constantly being made and broken, and chains are able to move and possibly form weak bonds with other chains.

### C. Drying

The recondensation of the silica gel happens shortly after water is removed in the last stage of the simulation (see Fig. 4). For dry gels with $N_{\text{water}}/N_{\text{Si}}$ equals 0.1, the connectivity increases, and the ratio $N_{\text{BO}}/N_{\text{Si}}$ rises above 1.1. This is consistent with non-hydrated silicate glasses having a high BO/Si ratio of 2 that corresponds to a $Q_4$ dominated structure. The formation of siloxane bonds may release a water molecule [41], which can be removed during the GCMC step. The reduction of the connectivity for high concentration of water indicates that the role of water is essential. We found that equilibrium is reached more rapidly in systems with high water concentrations. This indicates that water also plays the role of a catalyst in the process of gelation, in agreement with previous simulations [23]. The reduction of the fluctuations of $Q_n$ also indicates that low concentration of water diminishes the speed of the gelation. At higher concentration of water, the chains, being shorter, have more mobility, which enhances their propensity to make and break bonds. The dried gel shows an increase of mostly $Q_3$ which indicates that bonds are formed between several silicate chains. In comparison, the amount of $Q_2$ is similar to the one in the conditions with $N_{\text{water}}/N_{\text{Si}}$ equals to 1. After drying, 27 rings have been formed, with 11 five-member rings then 6, 4, 5, and 1 of

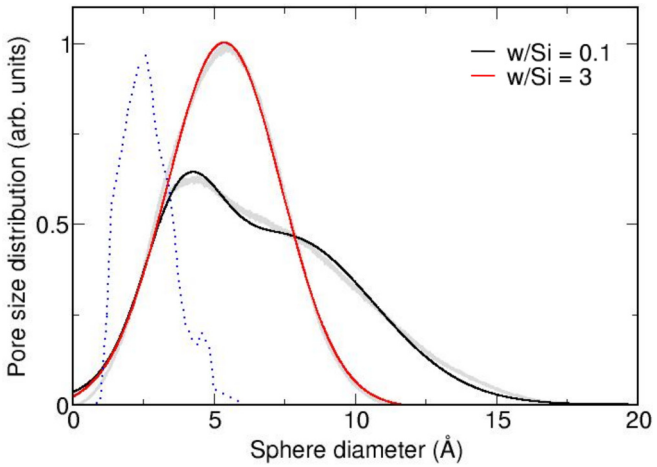


FIG. 5. Pore size distribution for a dry gel (black line) and a hydrated gel (red line) vs the sphere diameter used to evaluate pores size. Grey lines correspond to raw data, black and red lines are Gaussian fitting. Dotted lines are data, obtained by molecular dynamics, extracted from Rimsza and Du [26].

respectively four-, six-, three-, and seven-member rings. This is consistent with a glasslike structure.

A thin passivation gel layer that reduces its dissolution rate forms on hydrated glasses. This gel layer, at pH 7 to 9.5, is hardly hydrated and water is constrained in subnanometric pores [14]. The pore network is comparable to the gels we have simulated, in Fig. 5. For a hydrated gel with $N_{water}/N_{Si}$ ratio equals 2, we simulated, as shown in Fig. 4, that the silica chains are getting decondensed during dilution. However, for a dry gel, increasing the water to silicon ratio had no effect on the repartition of $Q_n$. The passivation is due to the formation of silica clusters formed by small silica rings of three to five members that are not affected by water hydrolisis [42]. Our simulations indicate that the thin layer dries quickly and therefore forms a glasslike structure, which is consistent with a self-healing mechanism [14].

### D. Comparison with experiments

In one of the founding experimental works on silica gels of Maciel and Sindorf [43], the authors have shown that the ratios in pure silica gels are roughly 21.7% of $Q_3$, 18.8% of Q4, and 6.3% of $Q_2$. Compared to our results, shown in Fig. 4, this would correspond to a dry gel, with a low ratio of water to silicon content. To the extent that, as mentioned by the authors, CP/MAS technique was used to probe the surface properties that are the most likely subject to drying, our results are consistent with these experiments. At high water content ($N_{water}/N_{Si}$ higher than 3), experiments [44,45] and our simulations indicate that $Q_1$ and $Q_2$ are dominating in pure silica gels. The initial gel structure we obtained has ratios $Q_1/Q_2 \approx 3/4$ and $Q_3/Q_2 \approx 1/2$ comparable to those of experiments ($Q_1/Q_2 \approx 2/3$ and $Q_3/Q_2 \approx 1/3$) [44]. In Fig. 2 of Vega and Scherer [44], the authors show that the initial structure has considerably densified after only half an hour of a reflux that accelerates dehydration ($Q_3/Q_2 \approx 1.5$ and $Q_4/Q_2 \approx 1/2$). In this experiment, the drying is well controlled by injection of $N_2$, therefore no side effects such as carbonation occur. The effect of drying we simulated is also well reproduced compared to those experiments ($Q_3/Q_2 \approx 1.2$ and $Q_4/Q_2 \approx 1/3$).

The authors note that a reflux of half an hour corresponds to an aging of 10 hours at ambient conditions. Our simulations are able to quickly reproduce the effect of drying observed experimentally over time. The combined simulation of the gelation, the dilution and the drying of the silica gel is 60 000 time steps. That number corresponds to a fictive time of 300 ps. Considering a fastening of the simulation by two orders of magnitude compared to molecular dynamics, the equivalent in simulation time is at least 30 ns.

The dry gel that has been simulated, with a ratio $N_{water}/N_{Si}$ of 0.1 has elastic properties, calculated by box deformation technique and using CSH-FF [46], of 0.8 GPa for the bulk modulus, 0.2 GPa for the shear modulus, 0.12 for the Poisson's ratio and the density is about 1.02. This silica gel is softer than for instance calcium-silicate-gels in cement that have a bulk modulus of about 70 GPa [47]. In aerogels and xerogels, having a density of 1.0, the experimental and calculated bulk modulus close is close to 5 GPa [48,49], which is comparable to the value we have calculated. The elastic properties of silica gels also depend on their chemical composition, hydration levels and pore size distribution.

To calculate the porosity, all water molecules were removed. The pore size distribution and volume were calculated using a method that consist of growing a sphere until the edge overlaps with an atom [50]. For that, a random position is drawn and used as the center of a growing sphere. The process is repeated 500 000 times and each sphere diameter is recorded to plot the histogram in Fig. 5. For the gel with $N_{water}/N_{Si}$ equal 3, the porosity is 0.31% (total pore volume of about 3500 Å$^3$) for a gel with $N_{water}/N_{Si}$ equal 0.1, the porosity is 0.26% (total pore volume of about 4000 Å$^3$). In Fig. 5, for the wet gel, the pore size distribution is a Gaussian centered on 5.37 Å with a half-size of 4.75 Å, whereas, for the dry gel, the pore size distribution can be fitted with two Gaussians centered on 3.84 and 7.32 Å and with a Sigma of 2.92 and 7.77 Å, respectively. The larger porosity shown by the driest gel is consistent with a more dense structure, having higher interconnectivity. Compared to previous simulations [26], our pores are wider, which indicates a higher densification of the silicates that corresponds to long simulation times. In Fig. 3 of Murder and Machin [51], the pore size distributions, measured by isotherms, indicate high number of pores around 0.6 nm, which is in agreement with our pore size distribution.

## IV. CONCLUSION

A method based on the coupling of grand canonical Monte Carlo and a brief parallel tempering was proposed. The structures that were obtained for the silica gel are in agreement with previous simulations. Noteworthy, the early formation of gels is quicker by at least two orders of magnitude using brief-PT compared to classical molecular dynamics. Therefore we were able to simulate long processes such as the gelation of a silica gel, its dilution and drying. These results were confronted to experiments; the interconnectivity in simulated silica gels corresponds to the one observed experimentally and depends on

the hydration levels. Since gels and glasses are structures out of the equilibrium that evolves over long periods of time, this method might become useful to predict long-time behavior of silica gels, alkali-silica gels, calcium-silicate-hydrate gels, etc. Beyond the scope of the present work, it will help to answer further questions such as how chemical attacks will change the gel structure, what is the role of cations in the solution or what is the effect of pH? The properties obtained on gels at the atomic scale are also being used for multiscale approaches to model gels [46,52,53]. This is an important step towards the understanding of gels and their manifold purposes.

## ACKNOWLEDGMENTS

R.D. wish to thanks CNRS and A*MIDEX foundation of AixMarseille University for support. This work was partly supported by the Natural Sciences and Engineering Research Council of Canada. We thank Compute Canada for generous allocation of computer resources.

[1] E. G. Vrieling, T. P. M. Beelen, R. A. van Santen, and W. W. C. Gieskes, Mesophases of (Bio)Polymer-Silica particles inspire a model for silica biomineralization in diatoms, Angew. Chem., Int. Ed. Engl. **41**, 1543 (2002).

[2] R. J.-M. Pellenq, A. Kushima, R. Shahsavari, K. J. Van Vliet, M. J. Buehler, S. Yip, and F.-J. Ulm, A realistic molecular model of cement hydrates, Proc. Natl. Acad. Sci. USA **106**, 16102 (2009).

[3] M. Olvera de la Cruz, A. V. Ermoshkin, M. A. Carignano, and I. Szleifer, Analytical theory and Monte Carlo simulations of gel formation of charged chains, Soft Matter **5**, 629 (2009).

[4] B. Lebeau, Silica-based materials for advanced chemical applications. By Mario Pagliaro, Angew. Chem., Int. Ed. Engl. **48**, 8405 (2009).

[5] D. Montarnal, M. Capelot, F. Tournilhac, and L. Leibler, Silica-like malleable materials from permanent organic networks, Science **334**, 965 (2011).

[6] T. Bhattacharjee, S. M. Zehnder, K. G. Rowe, S. Jain, R. M. Nixon, W. G. Sawyer, and T. E. Angelini, Writing in the granular gel medium, Sci. Adv. **1**, e1500655 (2015).

[7] K. Ioannidou, M. Kanduc, L. Li, D. Frenkel, J. Dobnikar, and E. Del Gado, The crucial effect of early-stage gelation on the mechanical properties of cement hydrates, Nat. Commun. **7**, 12106 (2016).

[8] R. Dupuis, J. S. Dolado, J. Surga, and A. Ayuela, Doping as a way to protect silicate chains in calcium silicate hydrates, ACS Sustainable Chem. Eng. **6**, 15015 (2018).

[9] T. Du, H. Li, G. Sant, and M. Bauchy, New insights into the sol-gel condensation of silica by reactive molecular dynamics simulations, J. Chem. Phys. **148**, 234504 (2018).

[10] L. Nguyen, M. Doblinger, T. Liedl, and A. Heuer-Jungemann, DNA-origami-templated silica growth by sol-gel chemistry, Angew. Chem., Int. Ed. Engl. **58**, 912 (2018).

[11] L. B. Skinner, S. R. Chae, C. J. Benmore, H. R. Wenk, and P. J. M. Monteiro, Nanostructure of Calcium Silicate Hydrates in Cements, Phys. Rev. Lett. **104**, 195502 (2010).

[12] J. Wang, P. V. A. Pamidi, and D. R. Zanette, Self-assembled silica gel networks, J. Am. Chem. Soc. **120**, 5852 (1998).

[13] P. Steins, A. Poulesquen, O. Diat, and F. Frizon, Structural evolution during geopolymerization from an early age to consolidated material, Langmuir **28**, 8502 (2012).

[14] S. Gin, P. Jollivet, M. Fournier, F. Angeli, P. Frugier, and T. Charpentier, Origin and consequences of silicate glass passivation by surface layers, Nat. Commun. **6**, 6360 (2015).

[15] M. J. Abdolhosseini Qomi, F.-J. Ulm, and R. J.-M. Pellenq, Evidence on the dual nature of aluminum in the calcium-silicate-hydrates based on atomistic simulations, J. Am. Ceram. Soc. **95**, 1128 (2012).

[16] P. J. M. Monteiro, S. A. Miller, and A. Horvath, Towards sustainable concrete, Nat. Mater. **16**, 698 (2017).

[17] D. W. Hobbs, *Alkali-Silica Reaction in Concrete* (Thomas Telford Publishing, 1988).

[18] D. Gebauer, M. Kellermeier, J. D. Gale, L. Bergstrom, and H. Colfen, Pre-nucleation clusters as solute precursors in crystallisation, Chem. Soc. Rev. **43**, 2348 (2014).

[19] M. H. Nielsen, S. Aloni, and J. J. De Yoreo, *In situ* TEM imaging of $CaCO_3$ nucleation reveals coexistence of direct and indirect pathways, Science **345**, 1158 (2014).

[20] X. Zhao, J. Kim, C. A. Cezar, N. Huebsch, K. Lee, K. Bouhadir, and D. J. Mooney, Active scaffolds for on-demand drug and cell delivery, Proc. Natl. Acad. Sci. USA **108**, 67 (2011).

[21] V. Mironov, T. Boland, T. Trusk, G. Forgacs, and R. R. Markwald, Organ printing: Computer-aided jet-based 3D tissue engineering, Trends Biotechnol. **21**, 157 (2003).

[22] S. E. Rankin, L. J. Kasehagen, A. V. McCormick, and C. W. Macosko, Dynamic Monte Carlo simulation of gelation with extensive cyclization, Macromolecules **33**, 7639 (2000).

[23] N. Z. Rao and L. D. Gelb, Molecular dynamics simulations of the polymerization of aqueous silicic acid and analysis of the effects of concentration on silica polymorph distributions, growth mechanisms, and reaction kinetics, J. Phys. Chem. B **108**, 12418 (2004).

[24] Y. Zhang, T. Li, D. Hou, J. Zhang, and J. Jiang, Insights on magnesium and sulfate ions adsorption on the surface of sodium alumino-silicate hydrate (NASH) gel: A molecular dynamics study, Phys. Chem. Chem. Phys. **20**, 18297 (2018).

[25] M. G. F. Angelerou, P. W. J. M. Frederix, M. Wallace, B. Yang, A. Rodger, D. J. Adams, M. Marlow, and M. Zelzer, Supramolecular nucleoside-based gel: Molecular dynamics simulation and characterization of its nanoarchitecture and self-assembly mechanism, Langmuir **34**, 6912 (2018).

[26] J. M. Rimsza and J. Du, Nanoporous silica gel structures and evolution from reactive force field-based molecular dynamics simulations, npj Materials Degradation **2**, 18 (2018).

[27] T. Ohkubo, S. Gin, M. Collin, and Y. Iwadate, Molecular dynamics simulation of water confinement in disordered aluminosilicate subnanopores, Sci. Rep. **8**, 3761 (2018).

[28] J. M. Rimsza and J. Du, Interfacial structure and evolution of the water-silica gel system by reactive force-field-based molecular dynamics simulations, J. Phys. Chem. C **121**, 11534 (2017).

[29] A. C. T. van Duin, S. Dasgupta, F. Lorant, and W. A. Goddard, ReaxFF a reactive force field for hydrocarbons, J. Phys. Chem. A **105**, 9396 (2001).

[30] G. M. Psofogiannakis, J. F. McCleerey, E. Jaramillo, and A. C. T. van Duin, ReaxFF reactive molecular dynamics simulation of the hydration of Cu-SSZ-13 zeolite and the formation of Cu dimers, J. Phys. Chem. C **119**, 6678 (2015).

[31] J. C. Fogarty, H. M. Aktulga, A. Y. Grama, A. C. T. van Duin, and S. A. Pandit, A reactive molecular dynamics simulation of the silica-water interface, J. Chem. Phys. **132**, 174704 (2010).

[32] D. J. Earl and M. W. Deem, Parallel tempering: Theory, applications, and new perspectives, Phys. Chem. Chem. Phys. **7**, 3910 (2005).

[33] R. H. Swendsen and J.-S. Wang, Replica Monte Carlo Simulation of Spin-Glasses, Phys. Rev. Lett. **57**, 2607 (1986).

[34] M. Sitarz, W. Mozgawa, and M. Handke, Rings in the structure of silicate glasses, J. Mol. Struct. **511-512**, 281 (1999).

[35] S. Sundararaman, L. Huang, S. Ispas, and W. Kob, New optimization scheme to obtain interaction potentials for oxide glasses, J. Chem. Phys. **148**, 194504 (2018).

[36] C. E. Bronnimann, R. C. Zeigler, and G. E. Maciel, Proton NMR study of dehydration of the silica gel surface, J. Am. Chem. Soc. **110**, 2023 (1988).

[37] X. Hou, R. J. Kirkpatrick, L. J. Struble, and P. J. M. Monteiro, Structural investigations of alkali silicate gels, J. Am. Ceram. Soc. **88**, 943 (2005).

[38] C. Balachandran, J. Munoz, and T. Arnold, Characterization of alkali silica reaction gels using Raman spectroscopy, Cement Concrete Res. **92**, 66 (2017).

[39] R. Dupuis, J. S. Dolado, J. Surga, and A. Ayuela, Tracing polymerization in calcium silicate hydrates using Si isotopic fractionation, J. Phys. Chem. C **122**, 8356 (2018).

[40] C. Benmore and P. J. Monteiro, The structure of alkali silicate gel by total scattering methods, Cement Concrete Res. **40**, 892 (2010).

[41] T. T. Trinh, A. P. J. Jansen, and R. A. van Santen, Mechanism of oligomerization reactions of silica, J. Phys. Chem. B **110**, 23099 (2006).

[42] T. Du, H. Li, Q. Zhou, Z. Wang, G. Sant, J. V. Ryan, and M. Bauchy, Atomistic origin of the passivation effect in hydrated silicate glasses, npj Materials Degradation **3**, 6 (2019).

[43] G. E. Maciel and D. W. Sindorf, Silicon-29 NMR study of the surface of silica gel by cross polarization and magic-angle spinning, J. Am. Chem. Soc. **102**, 7606 (1980).

[44] A. J. Vega and G. W. Scherer, Study of structural evolution of silica gel using 1H and 29Si NMR, J. Non-Cryst. Solids **111**, 153 (1989).

[45] F. Brunet, B. Cabane, M. Dubois, and B. Perly, Sol-gel polymerization studied through silicon-29 NMR with polarization transfer, J. Phys. Chem. **95**, 945 (1991).

[46] A. Dufresne, J. Arayro, T. Zhou, K. Ioannidou, F.-J. Ulm, R. Pellenq, and L. K. Béland, Atomistic and mesoscale simulation of sodium and potassium adsorption in cement paste, J. Chem. Phys. **149**, 074705 (2018).

[47] H. Manzano, J. S. Dolado, A. Guerrero, and A. Ayuela, Mechanical properties of crystalline calcium-silicate-hydrates: comparison with cementitious C-S-H gels, Phys. Status Solidi A **204**, 1775 (2007).

[48] T. Woignier, J. Pelous, J. Phalippou, R. Vacher, and E. Courtens, Elastic properties of silica aerogels, J. Non-Cryst. Solids **95-96**, 1197 (1987).

[49] J. S. Rivas Murillo, M. E. Bachlechner, F. A. Campo, and E. J. Barbero, Structure and mechanical properties of silica aerogels and xerogels modeled by molecular dynamics simulation, J. Non-Cryst. Solids **356**, 1325 (2010).

[50] S. Bhattacharya and K. E. Gubbins, Fast Method for Computing Pore Size Distributions of Model Materials, Langmuir **22**, 7726 (2006).

[51] R. J. Murdey and W. D. Machin, Adsorption hysteresis and the pore size distribution of a microporous silica gel, Langmuir **10**, 3842 (1994).

[52] K. Ioannidou, K. J. Krakowiak, M. Bauchy, C. G. Hoover, E. Masoero, S. Yip, F.-J. Ulm, P. Levitz, R. J.-M. Pellenq, and E. Del Gado, Mesoscale texture of cement hydrates, Proc. Natl. Acad. Sci. USA **113**, 2029 (2016).

[53] J. Arayro, A. Dufresne, T. Zhou, K. Ioannidou, J.-F. Ulm, R. Pellenq, and L. K. Béland, Thermodynamics, Kinetics, and Mechanics of Cesium Sorption in Cement Paste: A Multiscale Assessment, Phys. Rev. Materials **2**, 053608 (2018).